



Contents lists available at ScienceDirect

Bioorganic & Medicinal Chemistry

journal homepage: www.elsevier.com/locate/bmc



Vancomycin analogs: Seeking improved binding of D-Ala-D-Ala and D-Ala-D-Lac peptides by side-chain and backbone modifications

Siegfried S. F. Leung, Julian Tirado-Rives, William L. Jorgensen *

Department of Chemistry, Yale University, New Haven, CT 06520-8107, United States

ARTICLE INFO

Article history:

Received 30 April 2009

Revised 27 June 2009

Accepted 3 July 2009

Available online 10 July 2009

Keywords:

Vancomycin

Structure-based design

Free energy perturbation

Antibiotic resistance

ABSTRACT

In order to seek vancomycin analogs with improved performance against VanA and VanB resistant bacterial strains, extensive computational investigations have been performed to examine the effects of side-chain and backbone modifications. Changes in binding affinities for tripeptide cell-wall precursor mimics, Ac₂-L-Lys-D-Ala-D-Ala (**3**) and Ac₂-L-Lys-D-Ala-D-Lac (**4**), with vancomycin analogs were computed with Monte Carlo/free energy perturbation (MC/FEP) calculations. Replacements of the 3-hydroxyl group in residue 7 with small alkyl or alkoxy groups, which improve contacts with the methyl side chain of the ligands' D-Ala residue, are predicted to be the most promising to enhance binding for both ligands. The previously reported amine backbone modification as in **5** is shown to complement the hydrophobic modifications for binding monoacetylated tripeptides. In addition, replacement of the hydroxyl groups in residues 5 and 7 by fluorine is computed to have negligible impact on binding the tripeptides, though it may be pharmacologically advantageous.

© 2009 Published by Elsevier Ltd.

1. Introduction

Multi-drug resistant bacterial infections, such as those caused by methicillin resistant *Staphylococcus aureus* (MRSA), are a serious, global healthcare problem.¹ Recent data indicate that more deaths are now caused annually by MRSA infections than by HIV/AIDS in the United States.² Also known as the 'superbug', MRSA is resistant to many commonly used β -lactam antibiotics.³ The treatment of choice is usually vancomycin (**1**), a glycopeptide antibiotic which has a crosslinked heptapeptide scaffold and a disaccharide appendage that consists of D-glucose and L-vancosamine (Fig. 1a).⁴ Vancomycin interrupts cell-wall biosynthesis in gram-positive bacteria by binding to the D-Ala-D-Ala dipeptide terminus of the peptidoglycan cell-wall precursor.⁵ The strong binding interactions between vancomycin and the D-Ala-D-Ala dipeptide are characterized by five backbone-backbone hydrogen bonds.⁴ The resistance mechanism of the common vancomycin-resistant phenotypes, VanA and VanB, is to reprogram the D-Ala-D-Ala terminal sequence to the D-Ala-D-Lac depsipeptide upon exposure to vancomycin-type antibiotics, resulting in a 1000-fold decrease of the antibiotic activity.⁶

In response to the emergence of vancomycin-resistant bacterial strains, much effort is being directed to the development of second-generation glycopeptide antibiotics.⁷ A common approach in glycopeptide analog development is to apply semisynthetic modifications, including side chain and glycosidic substitutions, on the

existing glycopeptide antibiotics or their aglycon forms. Oritavancin and telavancin are two examples of semisynthetic second-generation glycopeptide antibiotics based on the vancomycin scaffold.^{8,9} Many of the semisynthetic derivatives feature non-binding site modifications that do not affect directly the interactions with the peptide termini of cell-wall precursors. For example, oritavancin is active against VanA strains, but its binding affinities for cell-wall precursor mimics with D-Ala-D-Ala (**3**) and D-Ala-D-Lac (**4**) sequences remain very similar to those of vancomycin.⁸

The non-binding site modifications are usually made at the termini of the heptapeptide core or on the carbohydrate. Hydrophobic substitutions on the vancosamine have been demonstrated to enhance antibacterial activity by promoting dimerization of the glycopeptide and by enabling the analog to anchor into the bacterial membrane.¹⁰ Dimerization appears to be beneficial due to resulting cooperative binding of the target ligands.^{10,11} A productive approach has been to link covalently vancomycin derivatives at the C-termini or through the sugar motifs.¹² The membrane anchoring has been suggested to be bactericidal by causing membrane permeation and depolarization.^{7j} The addition of an amino sugar unit at residue 6, as in oritavancin and chloroeremomycin, has been shown to be beneficial as well to overcome vancomycin resistance by promoting the dimerization of the analogs.^{10a,11c} Alternatively, Ge et al. have shown that chlorobiphenyl substitution on the vancosamine is capable of restoring antibacterial activity of an inactive vancomycin derivative, which has a damaged carboxylate-binding motif lacking residue 1.^{7b} This finding demonstrates that the transglycosylation process of peptidoglycan biosynthesis may be directly interfered with using modified glycopeptides.^{5d,13} Another

* Corresponding author. Tel.: +1 203 432 6278; fax: +1 203 432 6299.

E-mail address: william.jorgensen@yale.edu (W.L. Jorgensen).

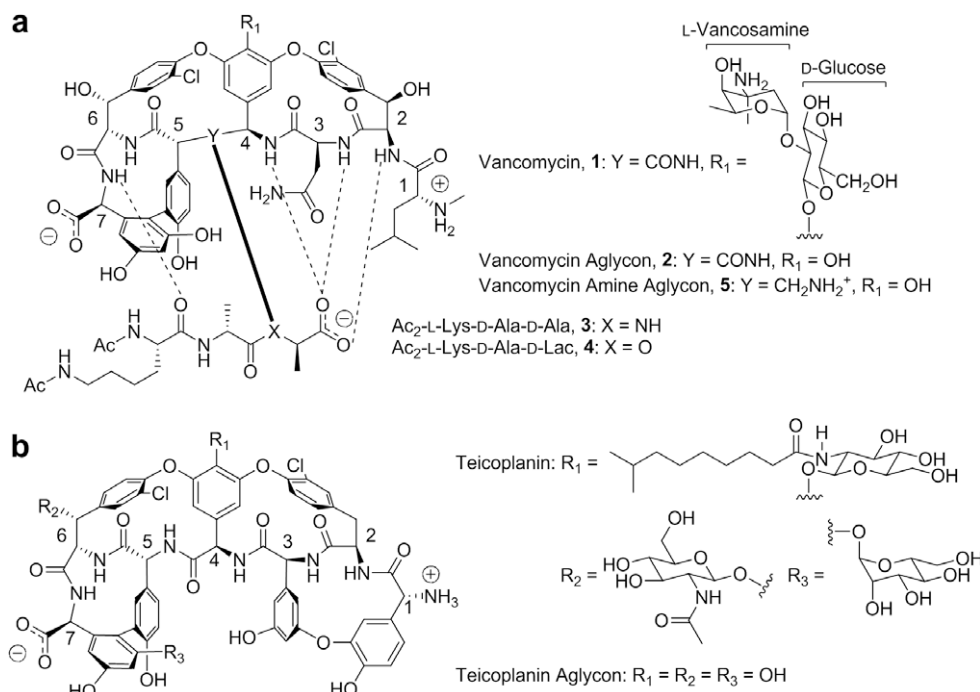


Figure 1. (a) Vancomycin (**1**), its aglycon (**2**), amine analog (**5**), and the tripeptide cell-wall precursor mimics (**3**, **4**). Potential hydrogen-bonding interactions are highlighted for the complex, (b) teicoplanin and its aglycon.

benefit of hydrophobic substitutions is that they can improve the pharmacokinetic and pharmacodynamic properties of glycopeptide analogs for more effective clinical treatment.^{7,8} Alternatively, improvement in antibacterial activity can be achieved by bifunctional derivatives. For example, vancomycin derivatives that are covalently linked to a β -lactam antibiotic have shown superior antibacterial activities than their parents.¹⁴

Binding-site modifications have also been pursued to produce vancomycin mimics. McAtee et al. explored nitrile substitution of the carboxamide side chain of Asn3 in vancomycin and derivatives, and they found it generally to be detrimental.¹⁵ However, the theoretical investigation of Axelsen and Li predicted that the binding of the depsipeptide sequence can be enhanced by increasing the hydrophobicity of the residue-3 side chain, though this has not been tested by experiment.¹⁶ Recently, Crane and Boger have shown that small improvement in activity against a VanA strain can be achieved by substitutions at residue 1 that allow additional hydrogen bond formation with the ligand.¹⁷ Jia et al. have developed a series of active derivatives that feature a 16-membered macrocyclic ring with 4 peptide units that reconstitutes the carboxylate binding region of vancomycin.¹⁸

Modification of residues 1 and 3 of the heptapeptide core have also been explored for the closely related glycopeptide antibiotic, teicoplanin (Fig. 1b). Excluding the crosslinked residues 1 and 3, the rest of the heptapeptide core of teicoplanin aglycon is essentially identical to the corresponding residues of vancomycin except for residue 2, which lacks the β -hydroxyl group. Not unexpectedly, removal of residue 1 or both residues 1 and 3 of the teicoplanin core adversely affects antibacterial activity owing to modification of the critical C-terminal binding motif.^{7a,13,19} On the other hand, enhanced antibiotic activity can be achieved by some changes for these residues, including substituting D-Lys at residue 1 and L-Phe or L-Lys at residue 3 of the derivative with a C-terminal methyl ester.²⁰

Modifications at other residues of the heptapeptide scaffold have also been investigated. For example, Boger and co-workers have synthesized a derivative of the methyl ester of vancomycin

aglycon that is tetramethylated on the hydroxyl groups of residues 4, 6 and 7, and it shows improved activity against vancomycin-resistant *Enterococcus* strains.^{15,21} Other vancomycin analogs with methoxy groups on residue 7 may be prepared by mutasynthesis.²² Of particular note, Crowley and Boger synthesized the amine analog (VAA, **5**) with the peptide bond between residue 4 and 5 replaced by a secondary amine, removing the source of lone pair repulsion with the lactate ester oxygen (Fig. 1).²³ The binding affinity of **5** to the Ac₂-L-Lys-D-Ala-D-Lac cell-wall precursor mimic (**4**) is improved and its antibiotic activity against a VanA bacteria strain is enhanced significantly as well. However, its binding affinity for Ac₂-L-Lys-D-Ala-D-Ala (**3**) is lowered due to the removal of the hydrogen-bond accepting carbonyl.

While total synthesis and semi-synthesis of vancomycin analogs are now possible, extensive exploration of potential variations remains challenging due to the structural complexity.²⁴ Thus, we have directed computational efforts to seek productive modifications that may help accelerate the development process. In designing analogs to bind strongly to both D-Ala-D-Ala and D-Ala-D-Lac sequences, the difference in hydrogen-bonding character between D-Ala and D-Lac provides a fundamental obstacle since a hydrogen-bond donating group is replaced by a weak hydrogen-bond acceptor. Consequently, electrostatic interactions that favor the binding of one sequence are likely to be unfavorable for the other, as seen in the case of **5**. To identify promising backbone modifications for the critical peptide linkage between residues 4 and 5, the effects of backbone alternatives on the binding for the tripeptide cell-wall precursor mimics were previously examined by Monte Carlo/free energy perturbation (MC/FEP) calculations.²⁵ However, the best choices that merged for achieving acceptable binding affinities for both D-Ala-D-Ala and D-Ala-D-Lac sequences remained to be the original peptide (VA, **2**) and the amine linkages (VAA, **5**). Thus, the present theoretical investigations were undertaken to extend the exploration to side-chain modifications for VA and VAA. As in the previous study, relative free energies of binding have been computed for the tripeptide cell-wall precursor mimics **3** and **4** with the vancomycin derivatives using MC/FEP calculations. In

addition, motivated by the folded conformation of the acetylated Lys side chain of the bis-acetylated tripeptides observed in the prior simulations,²⁵ binding of vancomycin analogs to mono-acetylated tripeptide ligands were also assessed.

2. Computational methods

2.1. MC/FEP calculations

The desired quantity is the change in free energy of binding, $\Delta\Delta G_b$, for a given ligand X that arises from a change to the vancomycin host, $VA_i \rightarrow VA_j$.²⁵ This is computed using the thermodynamic cycle in Figure 2. Two FEP calculations are required: one for $VA_i \rightarrow VA_j$ in water and one for the complexes $X \cdot VA_i \rightarrow X \cdot VA_j$ in water. In order to compare the effects of the $VA_i \rightarrow VA_j$ change on the D-Ala and D-Lac containing ligands, **3** and **4**, only three FEP calculations are needed since the $VA_i \rightarrow VA_j$ perturbation does not have to be repeated. The $\Delta\Delta G_b$ values for the ligands are obtained using Eqs. 1 and 2, for example, for **3**, $\Delta\Delta G_b = \Delta G_{b(j/Ala)} - \Delta G_{b(i/Ala)} = \Delta G_{Ala} - \Delta G_{Apo}$.

The perturbations that were performed are summarized in Figure 3. Standard protocols, which previously yielded results in good accord with observed difference in free energies of binding for **3** and **4** with VA and VAA, were followed.²⁵ In general, no more than one C, N, or O atom is added or deleted in one FEP calculation, and for removal of hydroxyl groups, use of two perturbations, $OH \rightarrow F \rightarrow H$, improves precision. The MC/FEP calculations were carried out using MCPRO with the OPLS-AA force field.^{26,27} All calculations were carried out at 298 K in a 25-Å radius water cap containing about 2000 TIP4P water molecules using 11 windows of simple overlap sampling.^{28,29} Each window consisted of 20 million MC configurations of solvent-only equilibration, 25–75 million MC configurations of full equilibration, and 50 million MC configurations of averaging. For the 11 windows, the total computation time is 24 days on one 2.4 GHz Intel Xeon processor. All degrees of freedom for the solutes were sampled, while the TIP4P water molecules were kept internally rigid. The statistical uncertainties ($\pm 1\sigma$) for the computed free energy changes were estimated by the batch means method.³⁰ The uncertainty for property θ was obtained by Eq. 3, where $\langle \theta \rangle$ is the overall average, and θ_i is the average for the i th batch. Typically there were 20 batches ($m = 20$), each containing 2.5 million configurations.

$$\sigma^2 = \sum_i^m \frac{(\theta_i - \langle \theta \rangle)^2}{m(m-1)} \quad (3)$$

Initial coordinates for apo VA and the complexes were based on apo (1AA5) and bound (1FVM) crystal structures of vancomycin.^{31,32} A solvent-equilibrated VA structure was obtained from an MC simulation that covered 1 billion configurations in a periodic box of 1170 TIP4P water molecules. For apo **2**, the solvent-

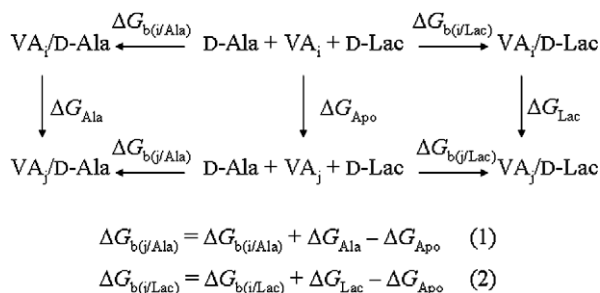


Figure 2. Thermodynamic cycle for MC/FEP calculations. VA_i and VA_j represent a pair of VA or VAA analogs; D-Ala and D-Lac represent **3** and **4**, respectively.

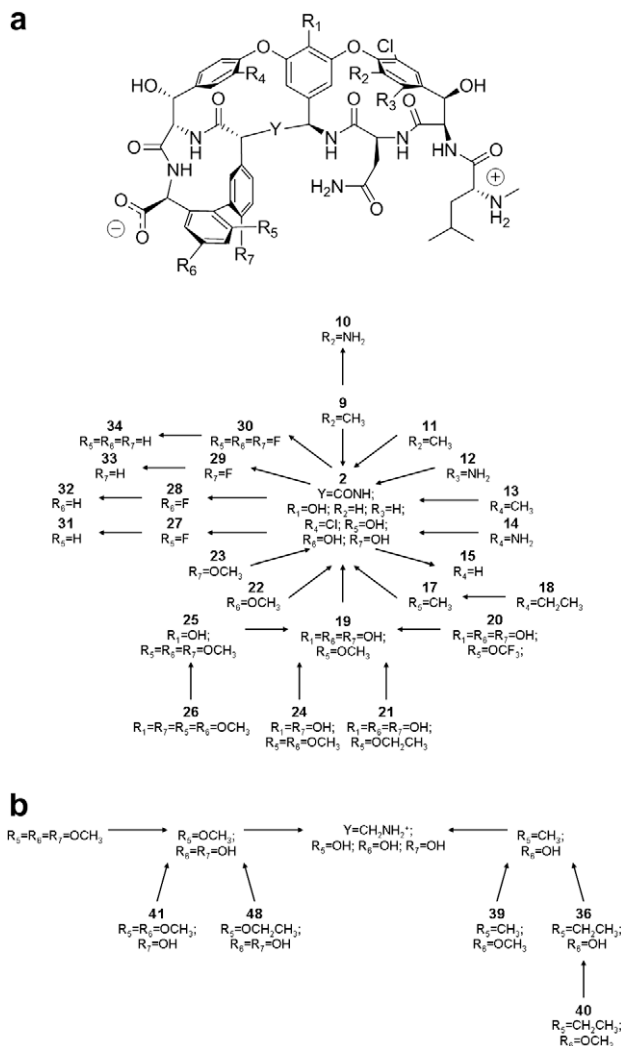


Figure 3. The MC/FEP schemes for examining vancomycin analogs. (a) The scheme for the analog series of VA (**2**), (b) the scheme for the analog series of VAA (**5**).

equilibrated structure provided the initial coordinates for the following MC/FEP calculations in the water caps. For the complexes, initial coordinates were obtained from the last configurations of the first (**2/3**) and the last (**2/4**) windows of the previous **2/3** → **2/4** FEP calculation.²⁵

For the series of VAA (**5**) analogs, the initial apo coordinates were obtained from an analogously solvent-equilibrated structure. Similarly, the D-Ala → D-Lac perturbation was performed with the bound complex **5/3** to obtain starting structures for the complexes **5/3** and **5/4**. For the calculations with monoacetylated ligands, the terminal acetamide (NHCOCH₃) of the Lys residue was replaced with a protonated ammonium group, NH₃⁺. As illustrated in Figure 1, all vancomycin derivatives were configured as zwitterions, so their N-terminal amine was protonated and the C-terminal carboxylate were deprotonated. Thus, the net charges for the VA and VAA analogs were 0 and 1. All tripeptide ligands were configured to have acetylated N-termini and deprotonated C-termini. Depending on the Lys residue, the net charge of the ligand was either −1 (Ac₂-Lys) or 0 (Ac-Lys).

2.2. Multi-solute interactive copies (MUSIC) simulations

In order to identify regions of the bound complexes that favor hydrophobic interactions, MULTI-Solute Interactive Copies (MUSIC)

simulations were performed on the VA complexes with ligands **3** and **4** using BOSS.²⁶ A MUSIC simulation is essentially a MC-simulated annealing simulation that does not evaluate the solvent–solvent interaction energy terms. As a result, the solvent molecules (probes) in the simulation only interact with the solute, which is the bound complex in this case, without interacting with other probes. The initial solute coordinates were based on the starting structures of complexes **2/3** and **2/4** from the MC/FEP calculations. For the purpose of increasing the accessibility of the probe molecules, Leu1 of VA was replaced with an ethyl group and the Cl of residue 6 was replaced with H. The resulting derivative (**16**) is shown in Figure 4. Each modified complex was first solvated in a 18-Å radius sphere of OPLS-AA methane molecules. Each simulation was carried out using a sequence of three temperatures: 2 million MC configurations at 100 °C, 2 million MC configurations at 0 °C, 1 million MC configurations at –100 °C. Only the probe molecules were sampled. While the complexes were kept rigid during the simulations, the Lennard–Jones parameters, σ and ϵ , were scaled by a factor of 0.85 at 100 °C and a factor of 0.92 at 0 °C to allow more efficient sampling of the probes at the interaction surface.

3. Results and discussion

3.1. Modifications at residues 2 and 6 of VA

The initial strategy was to improve interactions with the common structural features of both the D-Ala-D-Ala and D-Ala-D-Lac sequences. Methyl and amino group substitutions were attempted on **2** at R₂, R₃, and R₄ in residues 2 and 6 (Fig. 3), hoping to introduce either hydrophobic contact with the methyl side chain of the D-Ala residue or an additional hydrogen bond with the ligand's carboxylate group. The predicted $\Delta\Delta G_b$ values in Table 1 are anchored to the experimental data for **2/3** and **2/4**.³³ An improvement in binding affinity is indicated by a more negative ΔG_b value relative to that of **2/3** or **2/4**, namely $\Delta\Delta G_b < 0$ kcal/mol for the binding of **3** and $\Delta\Delta G_b < 4.4$ kcal/mol for the binding of **4**.

In general, the methyl and amino substitutions for R₂–R₄ are predicted to be unconstructive. At residue 2, the attempted substitutions (**9**–**12**) yield at least 1 kcal/mol poorer binding of **3**. Similar results are obtained for **4** except the amino substitution at R₂ (**10**), which has the same binding affinity as that of **2**.

Methyl substitution at R₂ appears to yield a steric clash with the D-Ala methyl side chain instead of forming a favorable contact. The C...C distances found in the complexes of **9** are too short for optimal hydrophobic contact (Fig. 5a and b). On the other hand, a methyl group at R₃ (**11**) is probably too close to the ligand's C-terminus, introducing unfavorable shielding of the carboxylate group (Fig. 5c and d). Rotation of the phenyl ring is likely hindered by the ortho Cl.

The amino substitutions at R₂ and R₃ both appear to fulfill their intended role as a hydrogen-bond donor for the ligand's carboxyl-

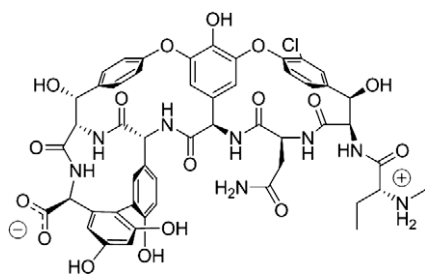


Figure 4. Vancomycin aglycon derivative **16** used in the MUSIC simulations.

Table 1

Calculated relative ΔG_b values for vancomycin analogs with modifications at residues 2 and 6

	R ₂	R ₃	R ₄	$\Delta\Delta G_b$ (kcal/mol)	
				3 (D-Ala-D-Ala)	4 (D-Ala-D-Lac)
2 ^a	H	H	Cl	(0.0)	(4.4)
9	CH ₃	H	Cl	3.0 ± 0.1	6.9 ± 0.1
10	NH ₂	H	Cl	1.8 ± 0.1	4.5 ± 0.2
11	H	CH ₃	Cl	0.9 ± 0.2	7.5 ± 0.2
12	H	NH ₂	Cl	1.0 ± 0.2	5.8 ± 0.2
13	H	H	CH ₃	0.2 ± 0.1	4.3 ± 0.1
14	H	H	NH ₂	2.8 ± 0.1	7.3 ± 0.1
15	H	H	H	1.8 ± 0.1	5.7 ± 0.1

^a Ref. 33. Experimental data in parentheses.

ate group based on the short NH...O distances (<2.5 Å) observed from the simulations (Fig. 6). The amino groups of analogs **10** and **12**, as shown in Figure 6, are very well-hydrated in both apo and bound states owing to the solvent-exposed binding site. For R₃ = NH₂, there is also a hydrogen bond with the backbone NH of residue 2. Therefore, the desolvation penalties associated with the binding processes of these amine analogs are significant. The negative results for the amino substitutions at residue 2 suggest that the additional intermolecular hydrogen bonding in the complexes does not offset the dehydration penalty. For binding of **4**, it may also enhance the repulsion between the D-Lac oxygen and the C=O of residue 4. Compared to the O...O distance between the ester and carbonyl oxygens in **2/4** (3.7 Å), the average O...O distances for **10/4** (3.3 Å) and **12/4** (3.1 Å) are noted to be shorter.

At residue 6, the computed $\Delta\Delta G_b$ values for both ligands with the methyl substituted analog **13** are essentially the same as those for **2**. However, replacing the chlorine atom with an NH₂ (**14**) or hydrogen (**15**) at R₄ is predicted to adversely affect the binding of both ligands by ca. 3 and 2 kcal/mol, respectively. Since the methyl group and Cl atom are similar in size but have opposite electrostatic properties, the similar results for analogs **2** and **13** suggest that the main role of the R₄ substituent is to provide favorable van der Waals contact with the ligands. Thus, reducing the size of the substituent, as in **15**, is not helpful. This result agrees with findings from a previous study of a series of vancomycin-based derivatives, which demonstrated that the removal of the Cl atom at residue 6 reduces the antibacterial activity.³⁵ Introduction of the extra hydrogen-bond donor in **14** also does not improve binding of either ligand because the NH₂ group does not form a hydrogen bond with the ligands and the amino group is comparably hydrated in both the apo and bound states.

3.2. Results from the MUSIC simulations

As ligand binding is often promoted by enhancing hydrophobic interactions, such possibilities were sought. However, identification of a suitable position for hydrophobic substitutions in the shallow, polar, and solvent-exposed binding cleft of **2** is not obvious. Hence, MUSIC simulations were performed with methane as a probe to search systematically for regions of the bound

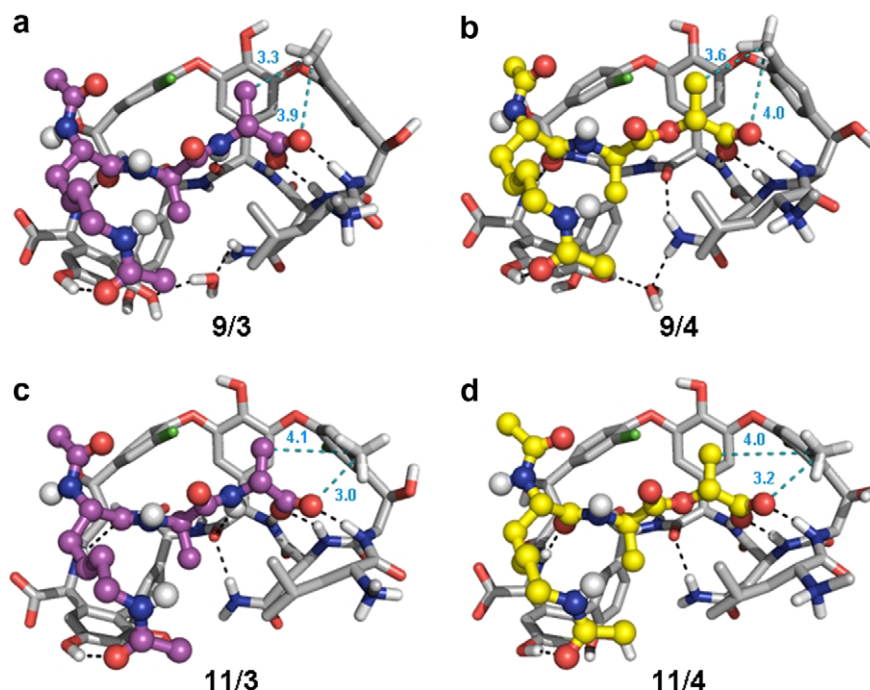


Figure 5. Representative complex structures of VA analogs with methyl substitutions at residue 2 from MC/FEP calculations. The VA analogs are shaded in gray; the tripeptide ligands are shown in ball and stick representations, **3** in purple and **4** in yellow; a few water molecules at the binding interface are included. Hydrogens on carbon are mostly not shown for clarity. Key hydrogen bonds are marked by black dashed lines. C...O and C...C distances between the methyl substituent and ligand are highlighted with cyan dashed lines. All distances are in Å. Structures were rendered using PyMOL.³⁴ (a) Complex **9/3**, (b) complex **9/4**, (c) complex **11/3**, (d) complex **11/4**.

complexes of VA that might benefit from increased hydrophobic interactions.

The last configurations of the complexes at -100°C from the MUSIC simulations are shown in Figure 7. The probes' interaction energies with both complexes at -100°C cover similar ranges, -3.3 to 0.8 kcal/mol for **3** and -3.3 to 0.7 kcal/mol for **4**. Since the solvent–solvent interactions are excluded, clustering of methane probes indicates an area of the complex that favors non-polar interactions. The ten methane probes that have the most negative interaction energies with each complex are displayed in Figure 7c and d.

In each case, the probe with the most favorable interaction energy (marked in orange) resides underneath the methyl side chain of the D-Ala residue at the bottom of the complex. This is the region of methyl clustering that involves the Leu1 side chain of **2** and the ligand's side chains of the D-Ala and Ac₂-Lys. The MUSIC result is consistent with the suggestion by Axelsen and Li that the binding affinity of **2** with **4** may be increased by improving non-polar interactions with the methyl side chain of the D-Ala.¹⁶ Based on the strong preference of non-polar interaction in this region observed for both ligands, the notion of enhancing the non-polar contact with the common D-Ala residue was pursued. A caveat with this MUSIC-based analysis is that the dehydration of the complex by the probe has not been considered. For a rapid approach, this effect could be estimated using the GB/SA method to compute the associated change in free energy of hydration. Or, as done here, the effect is covered by the FEP calculations.

3.3. Modifications at residues 4, 5, and 7 of VA

For potential hydrophobic contact with the ligand's D-Ala residue, VA residues 1, 3, and 7 are particularly relevant. Considering the unconstructive results for methyl substitutions at residue 2, hydrophobic substitutions at residue 1 may result in similar unfavorable screening of the ligands' carboxylate groups. While the previous study suggested that Asn3 may be a promising site for

hydrophobic modification,¹⁶ the side chain of Asn3 is often engaged in a hydrogen bond with the C=O of residue 4 and forms part of the shell of the binding site (Fig. 5). In view of these considerations, the present analysis focused on modifications for residue 7. The computed relative binding affinities of the examined analogs are listed in Table 2.

Initially, the examined modifications included methyl (**17**), ethyl (**18**), methoxy (**19**), trifluoromethoxy (**20**), and ethoxy (**21**) substitutions for R₅. These substitutions yielded some improvements, more so for **4** than **3**. Methoxy substitution at R₅ (**19**) is the most promising with enhancements for the ΔG_b of **3** by 0.9 kcal/mol and the ΔG_b of **4** by 1.8 kcal/mol. According to snapshots from the simulations (Fig. 8a and b), the R₅ methoxy group participates in the clustering of the surrounding methyl groups, which buries the target methyl side chain. The reasonable, computed C...C distances support the nature of the favorable hydrophobic contact. Both the ethoxy (**21**) and trifluoromethoxy (**20**) analogs have very similar computed binding affinities as the methoxy analog **19**.

However, the ethoxy group extends further into the solvent regardless of the bound ligand (Fig. 8c and d). The resulting hydrophobic contact between the R₅ ethoxy group and the ligand is expected to be less optimal than that of the methoxy analog **19**. However, the trifluoromethoxy alternative **20** emerges as equally promising as its methoxy relative **19**. Furthermore, the computed binding affinities for the methyl (**17**) and ethyl (**18**) analogs are very similar, and their enhancements are less than that of **19**. These modifications are estimated to improve the binding of **4** by about 1 kcal/mol, but to have no effect on the binding of **3**. The hydroxyl or alkoxy oxygen at R₅ almost always participates in a water-bridged hydrogen bond with the amido group in the side chain of Asn3, while the purely hydrophobic methyl and ethyl analogs lack this feature.

While the methoxy substitution at R₅ was constructive in the calculations, the tetramethoxy analog, **26**, previously prepared by Boger and co-workers has been experimentally determined to

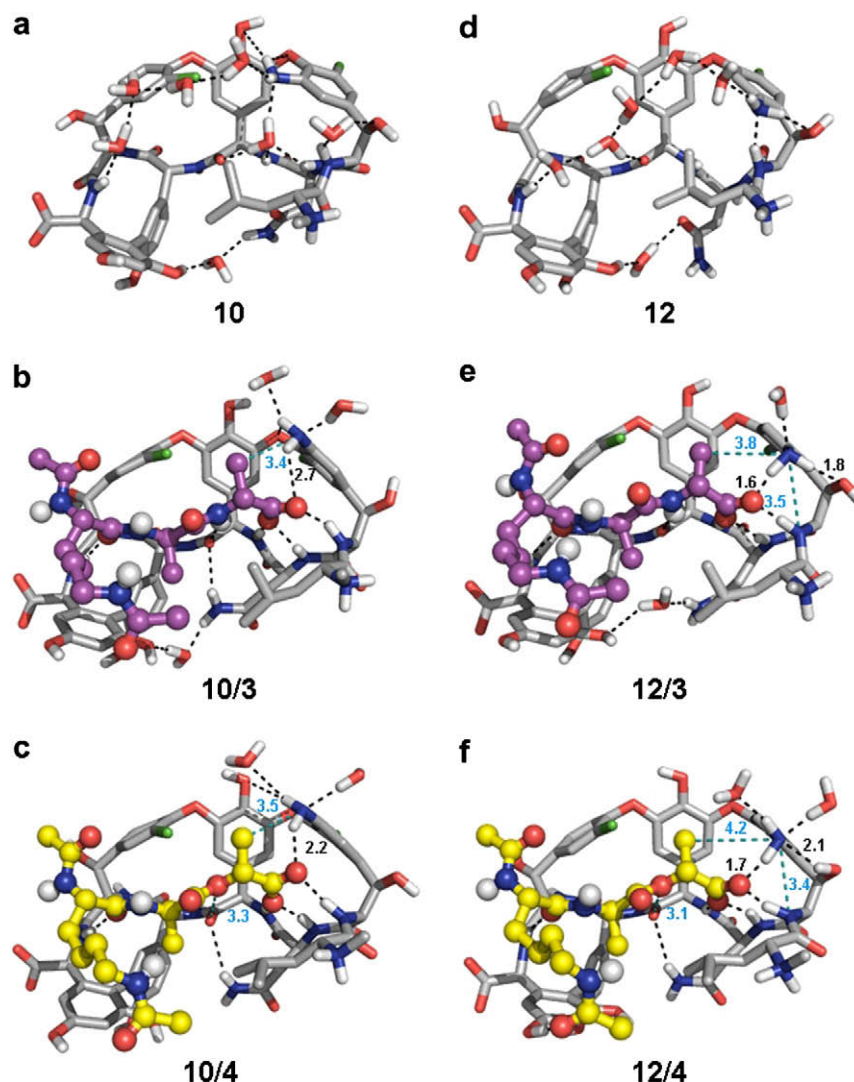


Figure 6. Representative complex structures of VA analogs with NH_2 substitutions at residue 2 from MC/FEP calculations. Some water molecules are included. Inter-molecular hydrogen bonds are marked with black dashed lines. The $\text{N}\cdots\text{C}$ and $\text{N}\cdots\text{N}$ distances (Å) are highlighted with cyan dashed lines. (a) Apo analog **10**, (b) complex **10/3**, (c) complex **10/4**, (d) Apo analog **12**, (e) complex **12/3**, (f) complex **12/4**.

yield no improvement in binding either tripeptide ligands, even though it shows enhanced *in vitro* activity.¹⁵ Motivated by this experimental finding, FEP calculations for methoxy substitutions at residues 4, 5 and 7 were performed. Contrary to the significant effect at R_5 , both methoxy substitutions at R_6 in residue 7 (**22**) and at R_7 in residue 5 (**23**) had negligible computed effect on the binding of either ligand. Methoxy substitution at R_6 may promote contact with the alkyl portion of the ligand's $\text{Ac}_2\text{-Lys}$ side chain, but this modification also disrupts the hydrogen bond with the $\text{Ac}_2\text{-Lys}$ terminal carbonyl group. For R_7 , the substituent is fully solvent-exposed and is not part of the binding interface, so methoxy substitution there also has no effect.

Polymethoxy-substituted possibilities substitutions, **24–26**, were then considered. The results suggest that the maximal enhancement can be achieved with the 3-methoxy (**19**) or 3,5-dimethoxy (**24**) analogs for residue 7. Additional methoxy substitutions at R_1 and R_7 are predicted to be unconstructive. The 3,5-dimethoxy analog **24**, which is illustrated in Figure 8e and f, is predicted to yield similar binding affinities for both ligands as the 3-methoxy analog **19**. The trimethoxy (**25**) and tetramethoxy (**26**) substitutions are predicted to be unconstructive for the binding of **3**, while having small but favorable effects on the binding of

4. The trimethoxy analog **25** does not show further enhancement over analogs **19** or **24** because the methoxy substitution at R_7 is not involved in binding interactions as for **23**. In agreement with the experimental finding, the tetramethoxy substitution is computed to be ineffective in enhancing the binding of either ligand.¹⁵ As shown in Figure 9, the R_1 methoxy substitution at residue 4 of analog **26** appears to be capable of forming favorable contact with the methyl side chain of the terminal residue of the ligand based on the reasonable $\text{C}\cdots\text{C}$ distance (4.2 Å). However, formation of this contact may adversely affect the hydration of nearby polar functionality in the complex. In any event, the only clear activity boost comes from methylation of the R_5 hydroxyl group in residue 7. Further methylation at R_6 is then benign and additional methylation of the R_1 or R_7 hydroxyl groups is counter-productive.

In order to explore further the importance of the hydroxyl groups at $\text{R}_5\text{--R}_7$, substitutions by fluorine and hydrogen were considered. Though hydrogen bonding with the ligands might be sacrificed, the increased hydrophobicity might be beneficial for binding. As reported in Table 2, fluorine substitutions at these positions actually have little impact. The only destabilization arises from substitution at R_6 yielding **28**, where the original OH group sometimes forms a hydrogen bond with the side-chain carbonyl

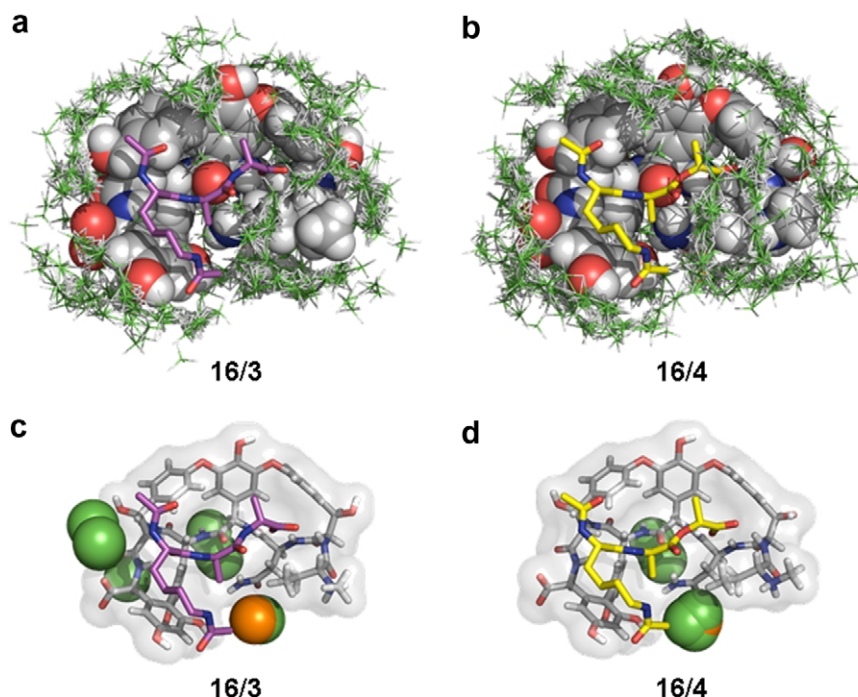


Figure 7. Representative structures from MUSIC simulations at $-100\text{ }^{\circ}\text{C}$. The bound complexes of **16** with **3** and **4** are shown in (a) and (b) with the methane probes located within $4\text{ }\text{\AA}$ of the complex. The analog **16** is shown in spheres with all atoms; the ligands (**3** in purple and **4** in yellow) are shown in sticks with heavy atoms only; the methane probes are represented in lines and are shaded in green. In (c) and (d), the same complexes of **16** are shown with the 10 probes that have the most favorable interaction energies for each complex. The carbon atoms of the probes are shown as green spheres except the one with the most favorable (negative) interaction energy is orange.

Table 2
Calculated relative ΔG_b values for vancomycin analogs with modifications at residues 4, 5 and 7

					$\Delta\Delta G_b$ (kcal/mol)	
	R ₁	R ₅	R ₆	R ₇	3 (D-Ala-D-Ala)	4 (D-Ala-D-Lac)
2 ^a	OH	OH	OH	OH	(0.0)	(4.4)
17	OH	CH ₃	OH	OH	-0.3 ± 0.1	3.5 ± 0.2
18	OH	CH ₂ CH ₃	OH	OH	0.1 ± 0.2	3.3 ± 0.2
19	OH	OCH ₃	OH	OH	-0.9 ± 0.3	2.6 ± 0.3
20	OH	OCF ₃	OH	OH	-0.7 ± 0.3	2.4 ± 0.3
21	OH	OCH ₂ CH ₃	OH	OH	-0.4 ± 0.3	2.1 ± 0.3
22	OH	OH	OCH ₃	OH	-0.2 ± 0.3	4.3 ± 0.3
23	OH	OH	OH	OCH ₃	-0.2 ± 0.3	5.1 ± 0.4
24	OH	OCH ₃	OCH ₃	OH	-1.2 ± 0.4	2.7 ± 0.4
25	OH	OCH ₃	OCH ₃	OCH ₃	1.0 ± 0.6	3.6 ± 0.5
26 ^b	OCH ₃	OCH ₃	OCH ₃	OCH ₃	(0.9) 1.0 ± 0.7	(4.6) 3.9 ± 0.6
27	OH	F	OH	OH	-0.1 ± 0.1	4.1 ± 0.1
28	OH	OH	F	OH	0.7 ± 0.1	5.2 ± 0.1
29	OH	OH	OH	F	0.1 ± 0.1	4.1 ± 0.1
30	OH	F	F	F	0.6 ± 0.2	4.5 ± 0.2
31	OH	H	OH	OH	0.6 ± 0.2	4.5 ± 0.2
32	OH	OH	H	OH	0.8 ± 0.2	5.6 ± 0.2
33	OH	OH	OH	H	0.8 ± 0.2	4.8 ± 0.2
34	OH	H	H	H	1.6 ± 0.2	5.5 ± 0.2

^a Ref. 33. Experimental data in parentheses.

^b Ref. 15.

group of the ligand's Ac₂-Lys residue. Relative to **2**, the ΔG_b values for **28** are predicted to increase by 0.7 and 0.8 kcal/mol for **3** and **4**. Fluorinations at R₅ and R₇, yielding **27** and **29**, result in similar binding affinities for both ligands as for VA **2**. In addition, the trifluoro analog **30** exhibits the same binding affinity for **4** as **2**, and its binding affinity for **3** shows minor degradation, 0.6 kcal/mol. On the other hand, complete removal of the hydroxyl groups in **31–34** is consistently unfavorable, though most losses in binding affinity are under 1 kcal/mol. With all three hydroxyl groups removed, the biphenyl analog **34** shows significant increases in ΔG_b , 1.6 and 1.1 kcal/mol. As illustrated by the chain of water molecules in Figure 10, the removal of the three substituents increases the solvent-accessibility of the binding cleft. Qualitatively, the striking results here are that the hydroxyl groups can be replaced by fluorines with little change in binding affinities, but possibly yielding pharmacological benefits, for example, via reduced metabolism.

Among the investigated modifications for **2**, substitutions at R₅ in residue 7 show the greatest effects on modulating the binding of peptides **3** and **4**. In summary, the order of computed ΔG_b values is:

3: OCH₃ \approx OCF₃ \approx OCH₂CH₃ \leq CH₃ < OH \approx F \approx CH₂CH₃ < H

4: OCH₂CH₃ \approx OCF₃ \approx OCH₃ < CH₂CH₃ \approx CH₃ < F < OH < H

The overall trends are similar with a preference for replacement of the R₅ hydroxyl group with a small alkoxy substituent. This improves hydrophobic interactions with the ligand, while retaining the role as a hydrogen-bond acceptor for a water molecule that bridges to the side-chain amido group of Asn3.

3.4. Modifications at residues 5 and 7 of VAA

Motivated by the positive results for modifications of **2**, similar changes were considered in residues 5 and 7 for VAA, **5**. The key issue is whether the gains would also apply to **5**, which shows

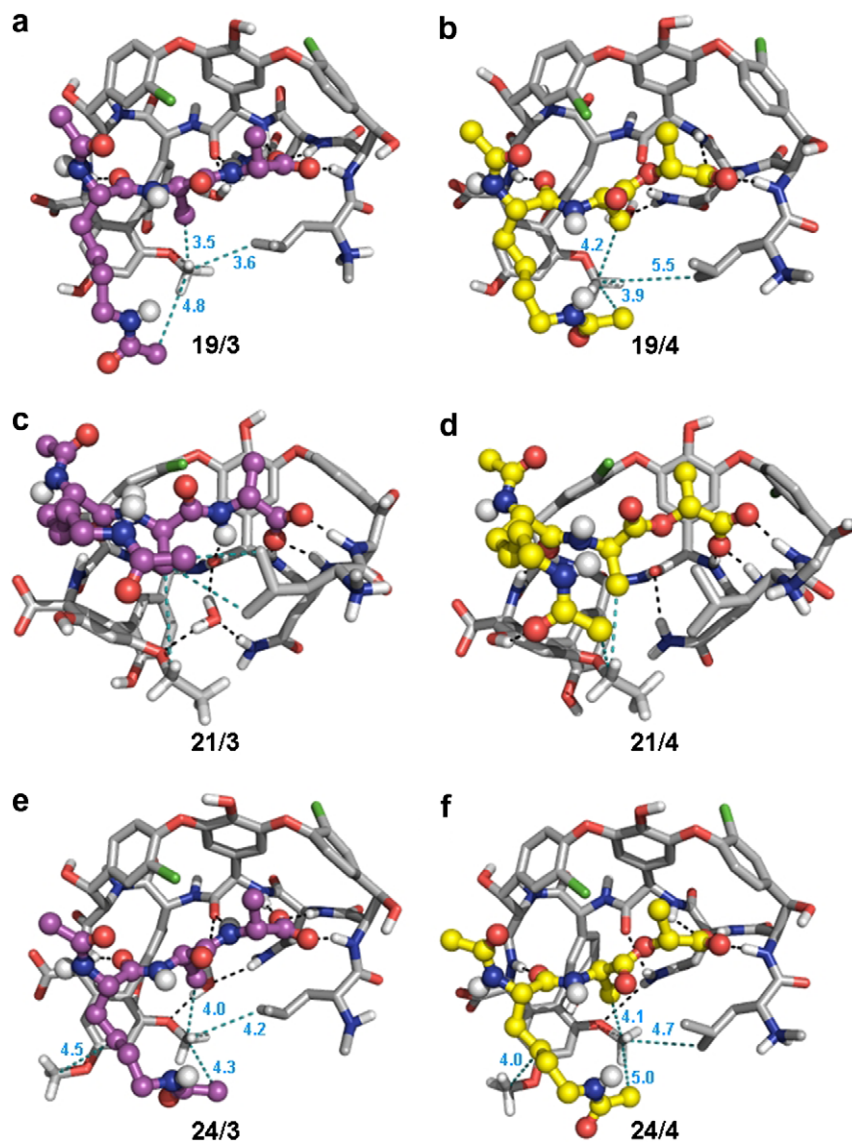


Figure 8. Representative structures of the bound methoxy (**19**), ethoxy (**21**), and dimethoxy (**24**) derivatives of VA. To highlight hydrophobic contacts, the C...C distances are marked by cyan dashed lines. Hydrogen bonds are highlighted by black dashed lines. (a) Complex **19/3**, (b) complex **19/4**, (c) complex **21/3**, (d) complex **21/4**, (e) complex **24/3**, (f) complex **24/4**.

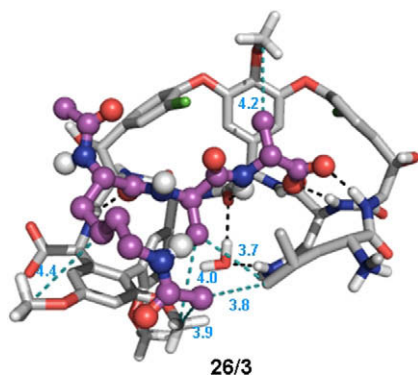
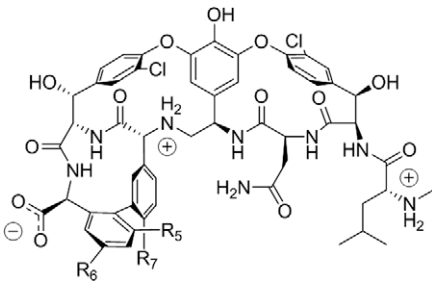


Figure 9. Representative structure of the bound complex of the tetramethoxy analog **26** with the D-Ala-D-Ala ligand, **3**. NH...O and C...C contacts (Å) are marked by black and cyan dashed lines.



Figure 10. Representative structure of the bound complex of the biphenyl analog **34** with the D-Ala-D-Lac peptide **4**. Removal of the hydroxyl groups from residues 5 and 7 of VA allows a water network to span the binding cleft. Hydrogen bonds are highlighted with dashed lines.

Table 3
Calculated relative ΔG_b values for derivatives of vancomycin amine aglycon (VAA)



	R ₅	R ₆	R ₇	$\Delta\Delta G_b$ (kcal/mol)	
				3 (D-Ala-D-Ala)	4 (D-Ala-D-Lac)
2	OH	OH	OH	(0.0) ^a	(4.4) ^a
5	OH	OH	OH	(2.1) ^b	(2.0) ^b 2.3 ± 0.1 ^c
35	CH ₃	OH	OH	1.6 ± 0.2	1.7 ± 0.2
36	CH ₂ CH ₃	OH	OH	1.9 ± 0.2	1.5 ± 0.2
37	OCH ₃	OH	OH	2.7 ± 0.3	1.1 ± 0.3
38	OCH ₂ CH ₃	OH	OH	3.5 ± 0.4	0.9 ± 0.3
39	CH ₃	OCH ₃	OH	0.4 ± 0.4	1.0 ± 0.3
40	CH ₂ CH ₃	OCH ₃	OH	2.9 ± 0.4	1.8 ± 0.4
41	OCH ₃	OCH ₃	OH	2.7 ± 0.5	0.5 ± 0.4
42	OCH ₃	OCH ₃	OCH ₃	2.9 ± 0.6	0.9 ± 0.6

^a Ref. 33. Experimental data in parentheses.

^b Ref. 23.

^c Ref. 25.

improved affinity for the D-Ala-D-Lac peptide **4**.^{23,25} The results are summarized in Table 3. In this case, methoxy substitution at R₅ in **5** yielding **37** is predicted to improve only the binding of peptide **4** but not of **3**. However, methyl substitution (**35**) improves the binding for both ligands, though it is computed to be somewhat less effective than methoxy substitution in enhancing the affinity for **4**. The computed $\Delta\Delta G_b$ value for the ethyl analog, **36**, is in between the results for the methyl and methoxy analogs for both ligands, while the ethoxy analog, **38**, is predicted to bind **4** well, but it is not favorable for **3**. Overall, all four substitutions yield improvements for **4**, while only the methyl and ethyl analogs yield better binding for **3**. The differences with the results for VA **2** must reflect changes in the binding site.

In order to illustrate the influence of the backbone variation on the binding site, the bound ethoxy analogs with different backbone linkages, **21** and **38**, are compared as an example in Figures 8c, d and 11. Due to the removal of the hydrogen-bond accepting carbonyl group between residues 4 and 5, the hydrogen bonding with the side-chain amido group of Asn3 or the surrounding water molecules is disrupted. Therefore, the Asn3 side chain in either complex with **38** is conformationally freer to rotate away from the

VAA backbone. Coupled with removal of the carbonyl group, the resultant void ends up being filled, at least partially, by the terminal methyl group of the ethoxy substituents, as illustrated in Figure 11. In contrast, the ethoxy group for **21** extends into the solvent (Fig. 8). The C...C distances between the ethoxy terminal carbon and the methylene carbon for **38** are ca. 5.7 Å, which is at least 1 Å shorter than the corresponding distances for **21**. However, the tighter packing may apply for both the bound and unbound states, so the net effect on binding is unclear, though the hydrophobic contact between the ethoxy group and the terminal acetyl methyl group of the Ac₂Lys residue seems improved in Figure 11.

Another aspect of the ligand binding process that needs to be considered is the conformation of the ligands' C-termini. In Figure 11, strong hydrogen bonding between the ligands' carboxylate groups and three backbone NH groups is apparent. Nevertheless, there are differences at the C-termini of **3** and **4** owing to the change in the preceding linkage from amide to ester. As illustrated in many complexes with **3**, the carboxylate group mostly stays in the same plane as the peptide bond, which reflects a favorable interaction with the peptide NH. Lacking this electrostatic attraction, the carboxylate group of **4** is freer to rotate. Thus, it is almost perpendicular to the plane of the ester linkage, when bound to **38** in Figure 11. On this basis, **4** can be expected to adapt better conformationally than **3** to optimize interactions in the binding site, which may help account for the uniform improvements for **4** in Table 3.

Some disubstituted VAA analogs were also modeled, as summarized in Table 3. The 5-methoxy,3-methyl analog **39** appears to be the most promising with improved affinities for both ligands by at least 1 kcal/mol. The 3,5-dimethoxy case (**41**), which is predicted to be constructive for both ligands with VA, shows substantial improvement, 1.5 kcal/mol, for the binding of **4**, but its affinity for **3** is somewhat weakened relative to **5**. The 3-ethyl,5-methoxy derivative **40** is found to be ineffective at enhancing the binding for either ligand. Similar to the results for VA, the additional methoxy group at residue 5 in the trimethoxy analog **42** does not yield improvement over the dimethoxy analog **41**.

Both analogs **39** and **41** can make favorable hydrophobic contacts with the D-Ala side chain of the ligands, as shown in Figure 12. The methyl substituent of analog **39** makes contact primarily with the D-Ala side chain, whereas the corresponding methoxy substituent of **41** appears to make favorable contact with both the D-Ala side chain and the terminal Ac₂-Lys methyl group. Another observation is that the bound ligands with **39** and **41** have a different hydrogen-bond pattern for the carboxylate-binding motif (Fig. 12e). In the absence of the carbonyl group in residue 4, both ligands shift towards the C-terminus of the VA analog, which shortens the distance between the carboxylate group and the protonated backbone amine.

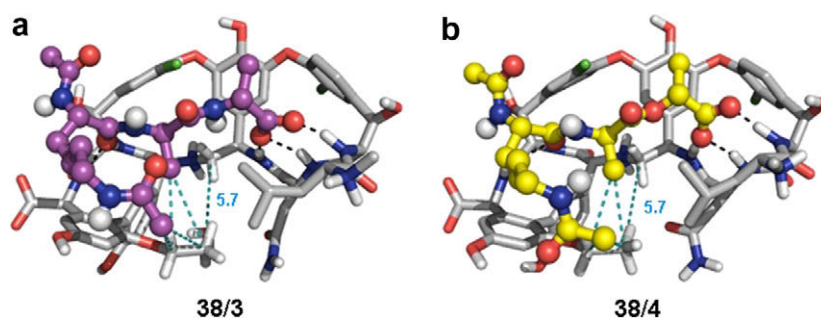


Figure 11. Representative structures of complexes of bound ethoxy derivatives (**38**) of VAA. The intermolecular hydrophobic contacts are highlighted by the corresponding C...C distances (Å). (a) Complex **38/3**, (b) complex **38/4**.

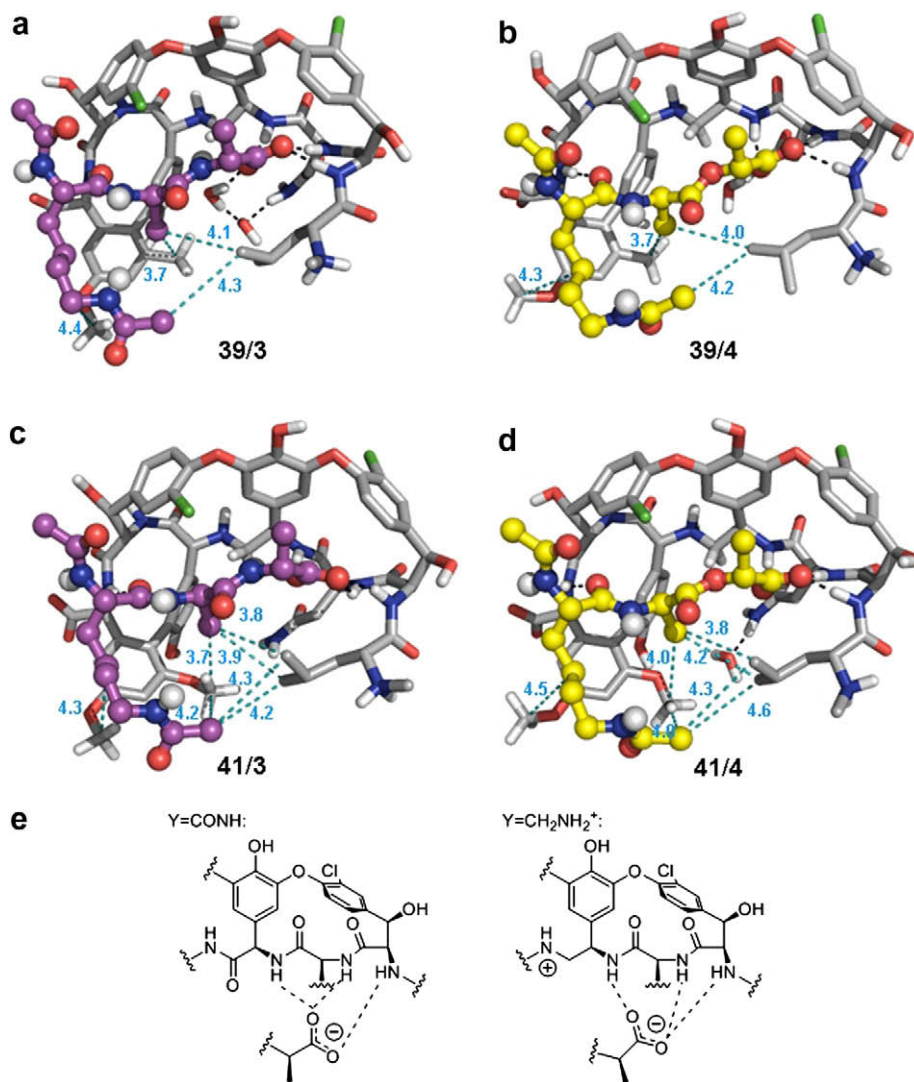


Figure 12. Representative structures of complexes with the 5-methoxy,3-methyl (**39**) and 3,5-dimethoxy (**41**) derivatives of vancomycin amine. Intermolecular contacts are marked by cyan dashed lines with C...C distances in Å. (a) Complex **39/3**, (b) complex **39/4**, (c) complex **41/3**, (d) complex **41/4**, (e) the change of hydrogen-bond pattern between the ligand's C-terminus and the amide NH groups of the carboxylate-binding motif.

3.5. Comparison of monoacetylated and diacetylated ligands

The proposed binding enhancements for modifications in residue 7 rely on favorable interactions with the nearby methyl groups, including those in the Leu1 side chain, the methyl side chain of the ligand's D-Ala residue, and the methyl terminus of the ligand's Ac₂-Lys side chain. While the diacetylated tripeptide

mimics have been used in previous experimental studies and in the present calculations, these ligands with Ac₂-Lys should be considered as mimics of crosslinked peptidoglycans after transpeptidation, which involves connecting two separate peptide termini by forming an isopeptide bond between the Lys side chain of one and the terminal D-Ala of the other (Fig. 13).^{5d} A non-crosslinked peptidoglycan is expected to have an unacetylated, protonated

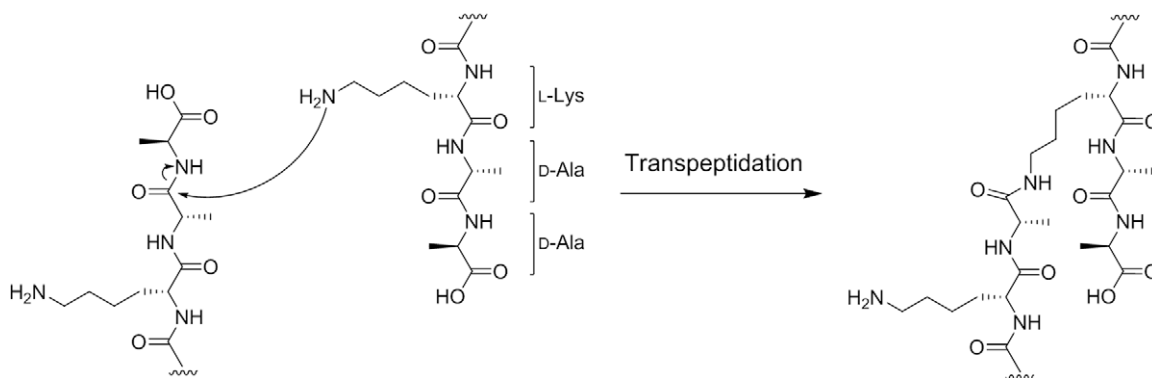


Figure 13. Crosslinking of peptide termini of peptidoglycan cell wall precursors through transpeptidation.

Lys residue. Although monoacetylated and diacetylated ligands are reasonable, alternative models, their binding interactions with vancomycin and its analogs are expected to be different.

In an early study, Nieto and Perkins showed that the binding affinity of diacetylated **3** to **1** is indeed 0.7 kcal/mol more favorable than that of the monoacetylated ligand, Ac-L-Lys-D-Ala-D-Ala (**43**).³⁶ The enhancement is assumed to be the result of the favorable methyl clustering that involves the Ac₂-Lys.²⁵ The protonated Lys side chain can be expected to adopt a conformation that extends into the solvent without interacting with Leu1.

In order to evaluate the proposed vancomycin analogs more comprehensively, monoacetylated ligands were examined as an alternative target, specifically, Ac-L-Lys-D-Ala-D-Ala (**43**) and Ac-L-Lys-D-Ala-D-Lac (**44**), where the Lys side-chain amine is now protonated. Analogs with three of the most promising modifications were studied, including methoxy, ethoxy, and dimethoxy substitutions at R₅ and R₆ in residue 7. In Table 4, the computed binding affinities are reported as $\Delta\Delta G_b$ relative to the original dihydroxy analogs, **2** or **5**. A negative $\Delta\Delta G_b$ value indicates an improvement in binding over **2** or **5**.

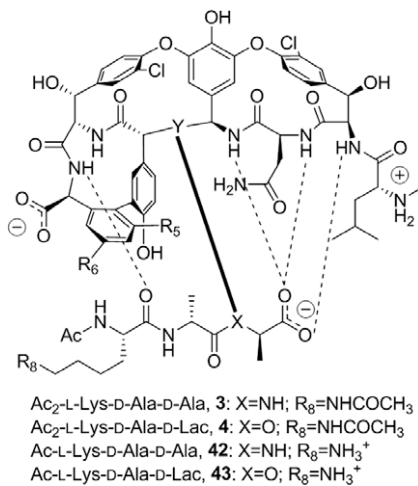
The favorable modifications on the original VA scaffold are found to be less effective for the monoacetylated ligands, **43** and **44**. Methoxy substitution at R₅ (**19**) is the only modification that improves the binding affinity for the D-Ala-D-Lac sequence regardless of the nature of the Lys residue in the ligand. However, the enhancement with **44** is 1 kcal/mol less than the improvement for **4**. As shown in Figure 14, the protonated Lys side chain of either monoacetylated ligand adopts an extended conformation, when bound to **19**, and is devoid of the favorable hydrophobic interaction with Leu1. The extended conformation also permits higher solvent accessibility to the binding interface, which can destabilize the binding interactions. Although all the modifications of **2** in Table 4 are predicted to improve the binding of **3**, only ethoxy substitu-

tion (**21**) is predicted to be beneficial for the binding of **43**. Notably, the dimethoxy substitution (**24**) is predicted to be unconstructive for both **43** and **44**.

In comparison, the results for the derivatives of VAA are more encouraging. All three of the attempted modifications are predicted to be constructive for the binding of both **43** and **44**, even though these modifications were originally predicted to be favorable only for the D-Ala-D-Lac sequence. The dimethoxy analog **41**, which emerges as the most promising in this series, is predicted to enhance the binding of **43** and **44** by 0.9 kcal/mol and 0.8 kcal/mol, respectively. Interestingly, 3-methoxy substitution (**37**) is computed to be more effective in improving the binding of **44** than of **43**, while ethoxy substitution (**38**) has the opposite effect. The improvements predicted for these analogs may be explained by the ligand readjustment, which is made in response to the backbone modification. The protonated Lys side chain of each monoacetylated ligand has an extended conformation that points into the solvent. Coupled with the reduction of the residue 4 carbonyl group, constraints on the ligand's binding orientation are diminished. The hydrophobic interaction between the Ac₂-Lys and Leu1 is also lost. In the case of **41**, ligand **43** (Ac-L-Lys-D-Ala-D-Ala) is shifted in the binding cleft in the absence of the hydrogen bond between Ac₂-Lys and residue 7 of the VA analog. Consequently, the methyl group of the first D-Ala residue may form hydrophobic contacts with Leu1, the R₅ methoxy group, and the methylene group of the modified linkage (Fig. 15a). This binding orientation would be impossible in the presence of the peptide linkage due to the hydrogen bond with the carbonyl group of residue 4. Furthermore, ligand **44** displays a radical change in position that alters the hydrogen-bonding pattern for its C-terminus. Without the hydrophobic attraction between the side chains, ligand **44** moves towards the center of the binding cleft (Fig. 15b) as compared to the bound ligand **4** with the same analog (Fig. 12d). The

Table 4

Calculated $\Delta\Delta G_b$ values for diacetylated (**3**, **4**) and monoacetylated ligands (**43**, **44**) with vancomycin aglycon (**2**), vancomycin amine aglycon (**5**), and their analogs



	Y	R ₅	R ₆	$\Delta\Delta G_b$ (kcal/mol) ^a			
				R ₈ = NHCOCH ₃		R ₈ = NH ₃ ⁺	
				3 (X = NH)	4 (X = O)	43 (X = NH)	44 (X = O)
2	CONH	OH	OH	0.0 ± 0.0	0.0 ± 0.0	0.0 ± 0.0	0.0 ± 0.0
19	CONH	OCH ₃	OH	−0.9 ± 0.3	−1.8 ± 0.3	0.1 ± 0.3	−0.8 ± 0.3
21	CONH	OCH ₂ CH ₃	OH	−0.4 ± 0.3	−2.3 ± 0.3	−0.6 ± 0.3	0.0 ± 0.3
24	CONH	OCH ₃	OCH ₃	−1.2 ± 0.4	−1.7 ± 0.4	1.4 ± 0.4	0.4 ± 0.4
5	CH ₂ NH ₂ ⁺	OH	OH	0.0 ± 0.0	0.0 ± 0.0	0.0 ± 0.0	0.0 ± 0.0
37	CH ₂ NH ₂ ⁺	OCH ₃	OH	0.6 ± 0.3	−0.9 ± 0.3	−0.2 ± 0.3	−0.7 ± 0.3
38	CH ₂ NH ₂ ⁺	OCH ₂ CH ₃	OH	1.4 ± 0.4	−1.0 ± 0.3	−1.3 ± 0.3	−0.2 ± 0.3
41	CH ₂ NH ₂ ⁺	OCH ₃	OCH ₃	0.6 ± 0.5	−1.5 ± 0.4	−0.9 ± 0.4	−0.8 ± 0.4

^a Relative to **2** or **5**.

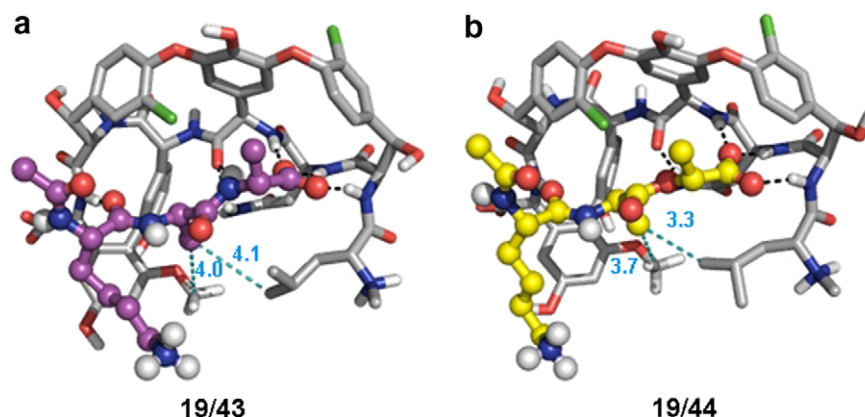


Figure 14. Representative structures of complexes of 3-methoxy analogs of vancomycin aglycon (**19**) with monoacetylated ligands containing protonated Lys residues, **43** and **44**. Intermolecular hydrophobic contacts are marked by cyan dashed lines and the corresponding C...C distances are reported in Å. (a) Complex **19/43**, (b) complex **19/44**.

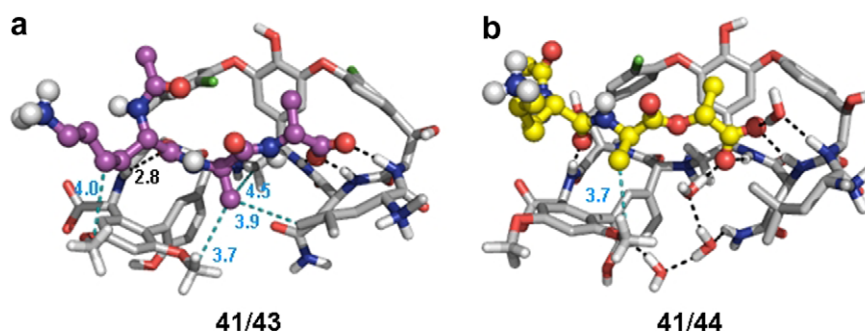


Figure 15. Representative structures of complexes of the 3,5-dimethoxy analog of VAA **41**, with monoacetylated ligands, **43** and **44**. The intermolecular hydrophobic contacts in the binding interface (C...C distances) are highlighted by cyan dashed lines and the hydrogen bonds (NH...O) are marked by black dashed lines. All distances are reported in Å. (a) Complex **41/43**, (b) complex **41/44**.

shift of the ligand and the rotation of the ligand's C-terminus free up enough room near the carboxylate group, so one water molecule can enter the binding interface to bridge between the backbone NH group of residue 2 and a carboxylate oxygen. A favorable contact between the methyl group of the D-Ala and the R₅ methoxy substituent is also noted (C...C distance = 3.7 Å). Thus, it seems reasonable that ligand **44** may achieve improved interactions with analog **41** due to the absence of the central carbonyl that repels the D-Ala-D-Lac sequence.

Based on the results for both sets of ligands, analog **41**, which has the amine linkage and 3,5-dimethoxy substitution at residue 7, emerges as the most promising vancomycin analog. Regardless of the form of the Lys residue, analog **41** exhibits enhancement for the binding of the D-Ala-D-Lac sequence and reasonable, if not improved, binding of the D-Ala-D-Ala sequence. The results also indicate that analogs with both backbone and side-chain modifications are more versatile than those with only backbone or side-chain modifications. A possible reason for this is that the beneficial effects of the side-chain substitutions are not strong enough to overcome the interactions between the ligand and the carbonyl group of residue 4, especially in the absence of the hydrophobic contacts between side chains of Ac₂-Lys and Leu1. As a result, the modification of the backbone carbonyl is required to enable greater effects for side-chain substitutions on the binding process.

4. Conclusions

The present investigation of vancomycin analogs with both side-chain and backbone modifications has provided a detailed

structure–activity analysis. Modifications at residues 2 and 6 intended to improve intermolecular contact or to introduce an additional hydrogen bond were not found to be constructive. Guided by MUSIC simulations, subsequent results indicated that, depending on the backbone of the vancomycin analog, enhancement may be achieved by methoxy or methyl substitutions at residue 7 that improve hydrophobic interactions with the D-Ala residue of both ligands. The binding of monoacetylated ligands was examined as well; dimethoxy substitution with the amine backbone modification (**41**) emerged as the most promising modification to improve binding of both monoacetylated and diacetylated ligands. The predicted binding enhancements are not large, which attests to the evolutionary optimization of vancomycin; however, the results indicate that experimental investigation of replacements of the hydroxyl groups of residue 7 by small alkyl and alkoxy groups is warranted. Replacement of the hydroxyl groups of residues 5 and 7 by fluorine may also be interesting from a pharmacological perspective.

The observed dependency of ligand binding on the acetylation and the conformation of the ligand's Lys residue reflects the limitation of the common model in which tripeptide ligands are used as the cell-wall precursor mimics. Although important insights on fundamental interactions can be obtained using models with only the essential dipeptide sequence, this simplification does not provide a complete picture of the binding interactions between the potential antibiotics and the cell-wall precursor termini.³⁷ Consequently, studies of these simplified systems may not be mirrored in experimental observations for corresponding bacteria.^{10,15,17} Overall, the present computational modeling has provided specific suggestions for new vancomycin analogs as well as insights into

the complexity of the binding interactions with vancomycin-type antibiotics and the challenges in discovery of improved antibacterial agents.

Acknowledgments

Gratitude is expressed to the National Institutes of Health (GM32136) and the National Foundation for Cancer Research for financial support and to Professor Dale L. Boger for helpful discussions and encouragement.

Supplementary data

Supplementary data associated with this article can be found, in the online version, at [doi:10.1016/j.bmc.2009.07.006](https://doi.org/10.1016/j.bmc.2009.07.006).

References and notes

- (a) Murray, B. E. *N. Engl. J. Med.* **2000**, *342*, 710; (b) Diekema, D. J.; BootsMiller, B. J.; Vaughn, T. E.; Woolson, R. F.; Yankey, J. W.; Ernst, E. J.; Flach, S. D.; Ward, M. M.; Franciscus, C. L. J.; Pfaller, M. A.; Doebbeling, B. N. *Clin. Infect. Dis.* **2004**, *38*, 78; (c) Deresinski, S. *Clin. Infect. Dis.* **2005**, *40*, 562; (d) Grudmann, H.; Aires-de-Sousa, M.; Boyce, J.; Tiemersma, E. *Lancet* **2006**, *368*, 877; (e) Gould, I. M. *Int. J. Antimicrob. Agents* **2007**, *30*, S66; (f) Rehm, S. J. *Cleve. Clin. J. Med.* **2008**, *75*, 177.
- Taubes, G. *Science* **2008**, *321*, 356.
- (a) Williams, D. H. *Nat. Prod. Rep.* **1996**, *13*, 469; (b) Ferber, D. *Science* **2003**, *302*, 1488.
- (a) Williamson, M. P.; Williams, D. H. *J. Am. Chem. Soc.* **1981**, *103*, 6580; (b) Harris, C. M.; Harris, T. M. *J. Am. Chem. Soc.* **1982**, *104*, 4293.
- (a) Reynolds, P. E. *Eur. J. Microb. Infect. Dis.* **1989**, *8*, 943; (b) Williams, D. H.; Bardsley, B. *Angew. Chem., Int. Ed.* **1999**, *38*, 1172; (c) Healy, V. L.; Lessard, I. A. D.; Roper, D. I.; Knox, J. R.; Walsh, C. T. *Chem. Biol.* **2000**, *7*, R109; (d) Kahne, D.; Leimkuhler, C.; Lu, W.; Walsh, C. *Chem. Rev.* **2005**, *105*, 425.
- (a) Bugg, T. D. H.; Wright, G. D.; Dutka-Malen, S.; Arthur, M.; Courvalin, P.; Walsh, C. T. *Biochemistry* **1991**, *30*, 10408; (b) Walsh, C. T.; Fisher, S. L.; Park, I. S.; Parhalad, M.; Wu, Z. *Chem. Biol.* **1996**, *3*, 21.
- (a) Malabarba, A.; Nicas, T. I.; Thompson, R. C. *Med. Res. Rev.* **1997**, *17*, 69; (b) Ge, M.; Chen, Z.; Onishi, H. R.; Kohler, J.; Silver, L. L.; Kerns, R.; Fukuzawa, S.; Thompson, C.; Kahne, D. *Science* **1999**, *284*, 507; (c) Malabarba, A.; Ciabatti, R. *Curr. Med. Chem.* **2001**, *8*, 1759; (d) Van Bambeke, F.; Van Laethem, Y.; Courvalin, P.; Tulkens, P. M. *Drugs* **2004**, *64*, 913; (e) Weist, S.; Süssmuth, R. D. *Appl. Microbiol. Biotechnol.* **2005**, *68*, 141; (f) Pace, J. L.; Yang, G. *Biochem. Pharmacol.* **2006**, *71*, 968; (g) Van Bambeke, F. *Curr. Opin. Invest. Drugs* **2006**, *7*, 740; (h) Liang, X.-T.; Fang, W.-S. *Medicinal Chemistry of Bioactive Natural Products*; John Wiley & Sons: Hoboken, 2006; (i) Wolter, F.; Schoof, S.; Süssmuth, R. D. *Top. Curr. Chem.* **2007**, *267*, 143; (j) Van Bambeke, F.; Mingeot-Leclercq, M. P.; Struelens, M. J.; Tulkens, P. M. *Trends Pharmacol. Sci.* **2008**, *29*, 124; (k) Donadio, S.; Sosio, M. *Curr. Top. Med. Chem.* **2008**, *8*, 654; (l) Křen, V.; Řezanka, T. *FEMS Microbiol. Rev.* **2008**, *32*, 1.
- Allen, N. E.; Nicas, T. I. *FEMS Microbiol. Rev.* **2003**, *26*, 511.
- (a) Judice, J. K.; Pace, J. L. *Bioorg. Med. Chem. Lett.* **2003**, *13*, 4165; (b) Pace, J. L.; Krause, K.; Johnston, D.; Debabov, D.; Wu, T.; Farrington, L.; Lane, C.; Higgins, D. L.; Christensen, B.; Judice, J. K.; Kaniga, K. *Antimicrob. Agents Chemother.* **2003**, *47*, 3602; (c) Leadbetter, M. R.; Adams, S. M.; Bazzini, B.; Fatheree, P. R.; Karr, D. E.; Krause, K. M.; Lam, B. M. T.; Linsell, M. S.; Nodwell, M. B.; Pace, J. L.; Wu, T. X.; Christensen, B. G.; Judice, J. K. *J. Antibiot.* **2004**, *57*, 326.
- (a) Allen, N. E.; LeTourneau, D. L.; Hobbs, J. N., Jr. *J. Antibiot.* **1997**, *50*, 677; (b) Sharman, G. J.; Try, A. C.; Dancer, R. J.; Cho, Y. R.; Staroske, T.; Bardsley, B.; Maguire, A. J.; Cooper, M. A.; O'Brien, D. P.; Williams, D. H. *J. Am. Chem. Soc.* **1997**, *119*, 12041.
- (a) Waltho, J. P.; Williams, D. H. *J. Am. Chem. Soc.* **1989**, *111*, 2475; (b) Gerhard, U.; Mackay, J. P.; Maplestone, R. A.; Williams, D. H. *J. Am. Chem. Soc.* **1993**, *115*, 232; (c) Mackay, J. P.; Gerhard, U.; Beauregard, D. A.; Westwell, M. S.; Searle, M. S.; Westwell, M. S.; Searle, M. S.; Williams, D. H. *J. Am. Chem. Soc.* **1994**, *116*, 4581; (d) Beauregard, D. A.; Williams, D. H.; Gwynn, M. N.; Knowles, D. J. C. *Antimicrob. Agents Chemother.* **1995**, *39*, 781.
- (a) Sundram, U. N.; Griffin, J. H.; Nicas, T. I. *J. Am. Chem. Soc.* **1996**, *118*, 13107; (b) Nicolaou, K. C.; Hughes, R.; Cho, S. Y.; Winsinger, N.; Smethurst, C.; Labischinski, H.; Endermann, R. *Angew. Chem., Int. Ed.* **2000**, *39*, 3823; (c) Jain, R. K.; Trias, J.; Ellman, J. A. *J. Am. Chem. Soc.* **2003**, *125*, 8740.
- Kerns, R.; Dong, S. D.; Fukuzawa, S.; Carbeck, J.; Kohler, J.; Silver, L.; Kahne, D. *J. Am. Chem. Soc.* **2000**, *122*, 12608.
- (a) Marquess, D.; Linsell, M. S.; Turner, D. S.; Trap, S. G.; Long, D. D.; Fatheree, P. R. U.S. Patent No. 687,868,6; (b) Long, D. D.; Aggen, J. B.; Christensen, B. G.; Judice, J. K.; Hegde, S. S.; Kaniga, K.; Krause, K. M.; Linsell, M. S.; Moran, E. J.; Pace, J. L. *J. Antibiot.* **2008**, *61*, 595; (c) Long, D. D.; Aggen, J. B.; Chinn, J.; Choi, S. K.; Christensen, B. G.; Fatheree, P. R.; Green, D.; Hegde, S. S.; Judice, J. K.; Kaniga, K.; Krause, K. M.; Leadbetter, M.; Linsell, M. S.; Marquess, D. G.; Moran, E. J.; Nodwell, M. B.; Pace, J. L.; Trapp, S. G.; Turner, S. D. *J. Antibiot.* **2008**, *61*, 603.
- McAtee, J. J.; Castle, S. L.; Jin, Q.; Boger, D. L. *Bioorg. Med. Chem. Lett.* **2002**, *12*, 1319.
- Axelsen, P. H.; Li, D. *Bioorg. Med. Chem.* **1998**, *6*, 877.
- Crane, C. M.; Boger, D. L. *J. Med. Chem.* **2009**, *52*, 1471.
- (a) Jia, Y.; Ma, N.; Liu, Z.; Bois-Choussy, M.; Gonzalez-Zamora, E.; Malabarba, A.; Brunati, C.; Zhu, J. *Chem. Eur. J.* **2006**, *12*, 5334; (b) Jia, Y.; Bois-Choussy, M.; Malabarba, A.; Brunati, C.; Zhu, J. *J. Antibiot.* **2006**, *59*, 543.
- Malabarba, A.; Ciabatti, M.; Maggini, M.; Ferrari, P.; Colomobo, L.; Denaro, M. *J. Org. Chem.* **1996**, *61*, 2151.
- Malabarba, A.; Ciabatti, R.; Gerli, E.; Ripamonti, F.; Ferrari, P.; Colombo, L.; Olsufyeva, E. N.; Pavlov, A. Y.; Reznikova, M. I.; Lazhko, E. I.; Preobrazhenskaya, M. N. *J. Antibiot.* **1997**, *50*, 70.
- McComas, C. C.; Crowley, B. M.; Hwang, I.; Boger, D. L. *Bioorg. Med. Chem. Lett.* **2003**, *13*, 2933.
- Weist, S.; Kittel, C.; Bischoff, D.; Bister, B.; Pfeifer, V.; Nicholson, G. J.; Wohlleben, W.; Süssmuth, R. D. *J. Am. Chem. Soc.* **2004**, *126*, 5942.
- Crowley, B. M.; Boger, D. L. *J. Am. Chem. Soc.* **2006**, *128*, 2885.
- (a) Evans, D. A.; Wood, M. R.; Trotter, B. W.; Richardson, T. I.; Barrow, J. C.; Katz, J. L. *Angew. Chem., Int. Ed.* **1998**, *37*, 2700; (b) Nicolaou, K. C.; Natarajan, S.; Li, H.; Jain, N. F.; Hughes, R.; Solomon, M. E.; Ramanjulu, J. M.; Boddy, C. N. C.; Takayanagi, M. *Angew. Chem., Int. Ed.* **1998**, *37*, 2708; (c) Nicolaou, K. C.; Jain, N. F.; Natarajan, S.; Hughes, R.; Solomon, M. E.; Li, H.; Ramanjulu, J. M.; Takayanagi, M.; Koumbis, A. E.; Bando, T. *Angew. Chem., Int. Ed.* **1998**, *37*, 2714; (d) Nicolaou, K. C.; Takayanagi, M.; Jain, N. F.; Natarajan, S.; Koumbis, A. E.; Bando, T.; Ramanjulu, J. M. *Angew. Chem., Int. Ed.* **1998**, *37*, 2717; (e) Boger, D. L.; Miyazaki, S.; Kim, S. H.; Wu, J. H.; Castle, S. L.; Loiseleur, O.; Jin, Q. *J. Am. Chem. Soc.* **1999**, *121*, 10004.
- Leung, S. S. F.; Tirado-Rives, J.; Jorgensen, W. L. *Bioorg. Med. Chem. Lett.* **2009**, *19*, 1236.
- Jorgensen, W. L.; Tirado-Rives, J. *J. Comput. Chem.* **2005**, *26*, 1689.
- Jorgensen, W. L.; Maxwell, D. S.; Tirado-Rives, J. *J. Am. Chem. Soc.* **1996**, *118*, 11225.
- Jorgensen, W. L.; Chandrasekhar, J.; Madura, J. D.; Impey, R. W.; Klein, M. L. *J. Chem. Phys.* **1983**, *79*, 926.
- (a) Lu, N.; Kofke, D. A.; Woolf, T. B. *J. Comput. Chem.* **2004**, *25*, 28; (b) Jorgensen, W. L.; Thomas, L. T. *J. Chem. Theory Comput.* **2008**, *4*, 869.
- Allen, M. P.; Tildesley, D. J. *Computer Simulations of Liquids*; Clarendon: Oxford, 1987.
- Loll, P. J.; Bevivino, A. E.; Korty, B. D.; Axelsen, P. H. *J. Am. Chem. Soc.* **1997**, *119*, 1516.
- Nitanai, Y.; Kikuchi, T.; Kakoi, K.; Hanamaki, S.; Fujisawa, I.; Aoki, K. *J. Mol. Biol.* **2009**, *385*, 1422.
- McComas, C. C.; Crowley, B. M.; Boger, D. L. *J. Am. Chem. Soc.* **2003**, *125*, 9314.
- DeLano, W. L. *The PyMOL Molecular Graphics System*, version 0.99; DeLano Scientific: Palo Alto, CA, 2006. <http://www.pymol.org>.
- Cooper, R. D. G.; Snyder, N. J.; Zweifel, M. J.; Staszak, M. A.; Wikie, S. C.; Nicas, T. I.; Mullen, D. L.; Butler, T. F.; Rodriguez, M. J.; Huff, B. E.; Thompson, R. C. *J. Antibiot.* **1996**, *49*, 575.
- Nieto, M.; Perkins, H. R. *Biochem. J.* **1971**, *123*, 789.
- (a) Kim, S. J.; Cegelski, L.; Preobrazhenskaya, M.; Schaefer, J. *Biochemistry* **2006**, *45*, 5235; (b) Cegelski, L.; Steuber, D.; Mehta, A. K.; Kulp, D. W.; Axelsen, P. H.; Schaefer, J. *J. Mol. Biol.* **2006**, *357*, 1253; (c) Kim, S. J.; Schaefer, J. *Biochemistry* **2008**, *47*, 10155.